BY-NC

Tomasz Ślęzak

Characteristics of MAG Welded Joints Made in Fine-Grained High-Strength Steel S960QL

Abstract: The paper presents the results of investigation performed in relation to butt welds made in steel S960QL using the MAG method. The research involved two types of welds, i.e. I (square butt weld preparation) and V-shaped. Metallographic tests enabled the determination of the HAZ area and helped identify structural changes in the heat affected zone. The neighbourhood of the fusion line revealed the presence of slight porosity. The analysis of the chemical composition of the HAZ and that of the weld indicated slight differences in their carbon equivalent values, indicating the proper selection of the filler metal. Microhardness tests indicated substantial differences of hardness between the fusion line and the weld. The weld characterised by square butt preparation revealed better characteristic.

Keywords: high-strength steel S960QL, MAG welding, weldability

DOI: *10.17729/ebis.2018.6/5*

Introduction

High-strength structural steels (HSS) are predominantly used in the fabrication of structural elements exposed to extreme loads. The high application potential of the above-named steels results from their high conventional yield point $R_{0.2}$ as well as from the favourable $R_{0.2}$–density ratio, i.e. the factor defining specific strength. For the aforementioned reasons, the high-strength structural steels are used in the structure of mining equipment elements exposed to heavy loads, telescopic extension arms of self-propelled cranes, pressure vessels or in special applications, e.g. spans of military bridge MS-20 [1-4]. The foregoing applications result not only from strength-related but also (if not primarily) economic aspects aimed to improve the effectiveness of the production process and increase the competitiveness of finished products. Advantages resulting from the use of high-strength steels make the latter very attractive. The increased strength of the structural material through the reduction of the cross-section of welded elements results in lighter structures. The reduction of the weld cross-section decreases costs related to the making and inspecting of welded joints as well as reduces welding process time. It should be noted that labour costs make up more than 70% of general welding-related costs. The load-bearing structure of the Tokyo Gate Bridge, opened in 2012, (Fig. 1) was made of special steel BHS700 having a yield point of at least 700 MPa, which made it possible to reduce the cost of bridge construction

mjr dr inż. Tomasz Ślęzak (Major PhD (DSc) Eng.) – Military University of Technology, Faculty of Mechanical Engineering, Institute of Mechanical Engineering, Warszawa;

BY-NC

by approximately 12% and open the bridge half a year earlier [5].

Fig. 1. Tokyo Gate Bridge [6]

Presently, the fabrication of steel structures combines various welding methods. Plasma, laser or electron beam welding methods are developed very intensively, yet the mass-scale production continues to be dominated by the metal active gas (MAG) welding. The widespread implementation of technologically advanced joining methods is primarily impeded by high costs of equipment investment as well as by the necessity of developing and implementing welding technologies in practice. The MAG method is characterised by significant versatility and flexibility. This method is easy to use in automated processes and does not require special equipment (e.g. vacuum chambers indispensable for electron beam welding). Welded elements can have almost any size and varied geometry. In addition, particularly as regards MMA welding, the method is characterised by significantly higher efficiency and lower weld fabrication costs [7].

Weldability of high-strength structural steels

One of the most important features of structural steels is their weldability. Approximately 2/3 of the global production of steel in the form of rolled products is subjected to joining, usually welding [8]. Weldability is the "ability of steel (subjected to welding) to form joints characterised by specific physical properties and capable of transferring specific loads provided for a given structure" (definition by J. Pilarczyk) [9]. The weldability of structural steels is assessed through the verification of obtained joint structure and hardness, the toughness of the weld and of the HAZ as well as hot and cold crack resistance etc. The above-named features are often difficult to combine and, in terms of structural steels having a yield point of 1 GPa, they exclude one another. The aforesaid limitation results from the permissible value of carbon equivalent depending on the content of carbon and that of alloying elements. This parameter is decisive for the hardenability of steel and, combined with susceptibility of the steel to crack formation in the HAZ, for steel weldability (Fig. 2).

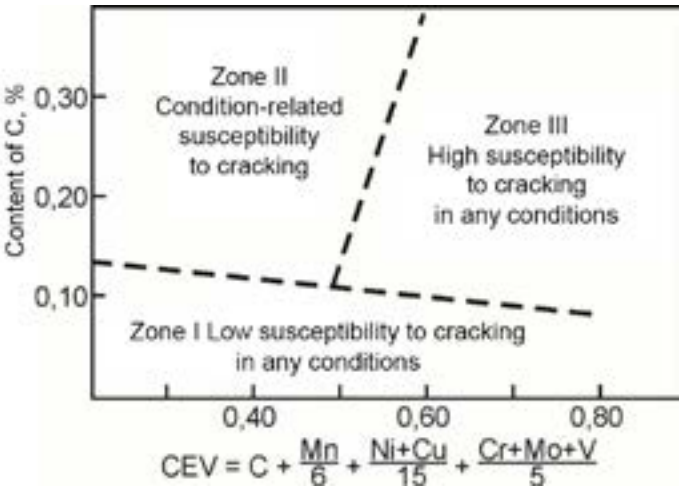

Fig. 2. Effect of the carbon content and carbon equivalent (CEV) on the susceptibility of steel with microagents to crack formation in the HAZ [10]

The refinement and structural stability are obtained by adding slight amounts of alloying elements such as niobium, titanium, vanadium or aluminium. The above-named elements combine carbon, affect the formation of stable carbides, nitrides and carbonitrides as well as delay or restrain the process of recrystallization (Fig. 3 and 4). The slight contents of carbon, manganese and alloying agents reduce hardenability and, consequently, improve weldability, leading to the obtainment of a structure characterised by very high toughness [11].

BY-NC

Weldability of high-strength toughened steel S960QL

Subject of research

The tests involved a 6 mm thick plate made of steel S960QL, known under commercial name SuperElso® 960 and manufactured by Industeel. The chemical composition and mechanical properties of the test steel are presented in Table 1. The structure-related test results are presented in Figures 5 and 6. The tests aimed to identify the chemical composition of the steel were performed using a Jeol JSM-6610 scanning electron microscope equipped with an EDS Oxford X-max X-radiation energy dispersive spectrometer. The mechanical properties were determined on the basis of tensile test (performed three times) using an Instron 8802 hydraulic pulsator equipped with a strain gauge having a basis of 50 mm. The value of carbon equivalent Ce was determined using dependence (1).

$$Ce = C + \frac{Mn}{6} + \frac{Cr + Mo + V}{5} + \frac{Ni + Cu}{15} \quad [\%] \tag{1}$$

The fractographic tests revealed the high plasticity of the test steel as well as its higher susceptibility to decohesion in the normal direction towards the surface (resulting from the rolling process and manifested by edges in the parallel arrangement.

The test joints of steel S960QL were made at Instytut Spawalnictwa in Gliwice. The tests involved the making of two types of butt-joints, i.e. with I-shaped and V-shaped weld grooves. The technological parameters of the welding process were adjusted in accordance with requirements related to the joining of fine-grained high-strength steel S960QL, paying particular attention to a heat input, which should not exceed 1 kJ/mm [12-13]. The joints were made using the MAG welding method. The welding process was shielded by an active gas mixture containing 82% CO_2 and 18% Ar (EN ISO 14175 - M21 - ArC - 18). The filler metal used in the tests was a UNION X96 (EN ISO 16834 - A - G Mn4Ni2,5CrMo) having a diameter of

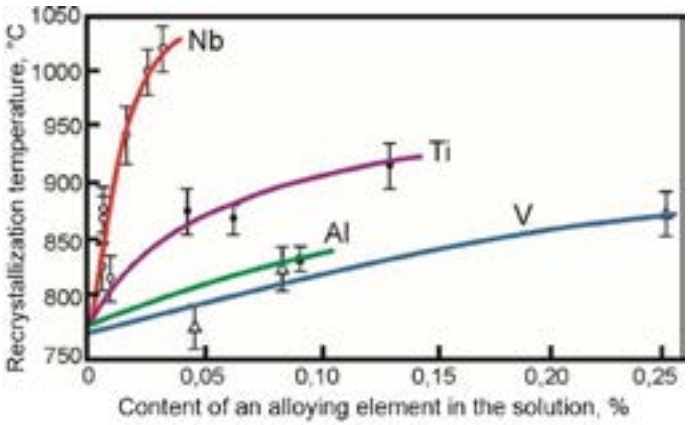

Fig. 3. Effect of the contents of microadditions soluble in austenite on the temperature of the recrystallization of steel containing 0.07% C, 1.40% Mn and 0.25% Si [10]

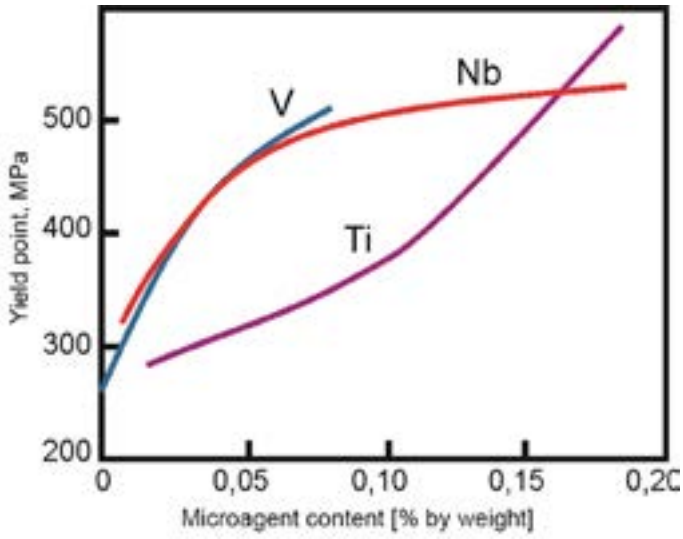

Fig. 4. Effect of Nb, Ti and V contents on the yield point of hot-rolled steel (own study based on [10])

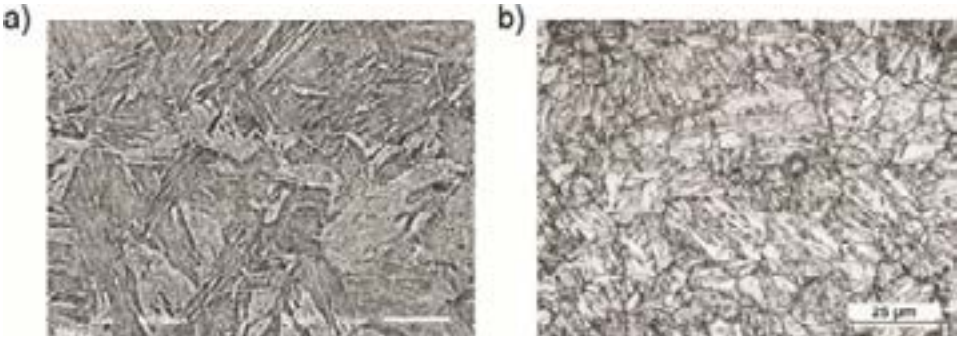

Fig. 5. Fine-grained martensitic-bainitic structure of steel S960QL observed using the scanning (a) and optical (b) microscope; etchant: Nital (3%)

BY-NC

Table 1. Chemical composition and mechanical properties of steel S960QL identified on the basis of an inspection certificate (A) and individual tests (B)

	Contents of alloying elements [%]								
	C	Mn	P	S	Si	Cu	Ni	Cr	Ce
A	018	112	0008	>0001	027	015	0077	022	0567
B	018[1)]	126	0008	-	035	017	0052	026	0585
	Mo	Al	Nb	V	Ti	B	N		
A	068	0078	0002	0027	0004	00028	0005		0567
B	061	0090	-	0032	0012	-	-		0585
Mechanical properties									
	Young's modulus E [MPa]	Yield point R_{02} [MPa]		Ultimate tensile strength R_m [MPa]		Elongation A [%]		Area reduction Z [%]	
A	-	997		1069		13		-	
B	219600	974		1070		142		456	

[1)] values according to the certificate

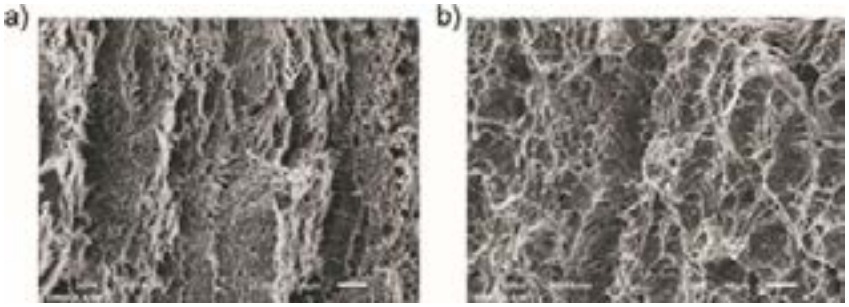

Fig. 6. Fractographic test results concerning the test specimens made in steel S960QL: after the tensile test (a) and after the impact test (b); (SEM)

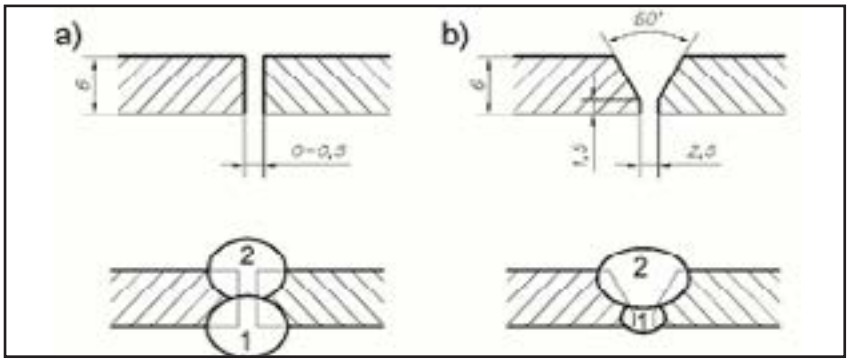

Fig. 7. Pre-weld preparation of edges and the welding sequence

Table 2. Chemical composition and mechanical properties of filler metal Union X96 [14]

Contents of alloying elements [%]						*Ce*
C	Mn	Si	Ni	Cr	Mo	
0,12	1,90	0,80	2,35	0,45	0,55	0,793
Mechanical properties						
Yield point $R_{p0.2}$ [MPa]	Ultimate tensile strength R_m [MPa]		Elongation A [%]	Toughness KCV [J/cm^2]		
				+20°C	-50°C	
930	980		14	80	47	

1.2 mm. The chemical composition and the mechanical properties of the filler metal are presented in Table 2 [14]. All of the joints were made in the flat position (PA). The primary welding process parameters are presented in Figure 3. Figure 7 presents the pre-weld preparation of the test plates and the welding sequence applied during the process.

Structural analysis of the welded joint

Figure 8 presents macroscopic photographs of both joint types. The metallographic tests performed on the cross-sectional metallographic specimens of the welded joints were performed using a SEM Jeol JSM-6610 microscope. Exemplary results related to the weld having the I-shaped weld groove are presented in Figure 9. The observations were carried out using SE and BSE detectors.

The fusion line area contained slight porosity, with gas pores having diameters restricted within the range of 0.5 µm to 1.5 µm. The HAZ

BY-NC

Table 3. Welding parameters

	Bead no.	Current [A]	Arc voltage [V]	Filler metal feeding rate [m/min]	Welding rate [mm/min]	Gas flow rate [l/min]	Linear energy [kJ/mm]
V-type	1	150	19.5	5.5	210	14	0.67
	2	260	27.0	7.5	450	14	0.75
I-type	1	260	27.0	7.5	450	14	0.75
	2	260	27.0	7.5	450	14	0.75

coarse-grained superheated area was up to 0.5 mm in width and contained grains having a diameter restricted within the range of 100 μm to 200 μm.

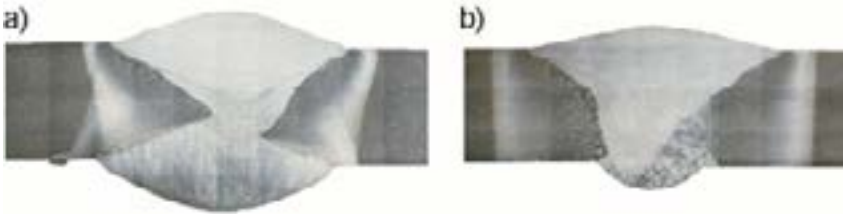

Fig. 8. Cross-sectional metallographic specimens of the I (a) and V-shaped weld (b) in steel S960QL

Analysis of the chemical composition of the fusion line

The chemical composition in the fusion line was identified using the EDS technique. The analysis was performed at five points, along a section of 500 μm containing the fusion line. The area subjected to measurements and XRD patterns obtained in the tests are presented in Figure 10. In turn, contents of chemical elements are presented in Table 4. The analysis concerned with the distribution of alloying elements was extended by surface analysis (the so-called mapping). The exemplary distribution of nickel is presented in Figure 11.

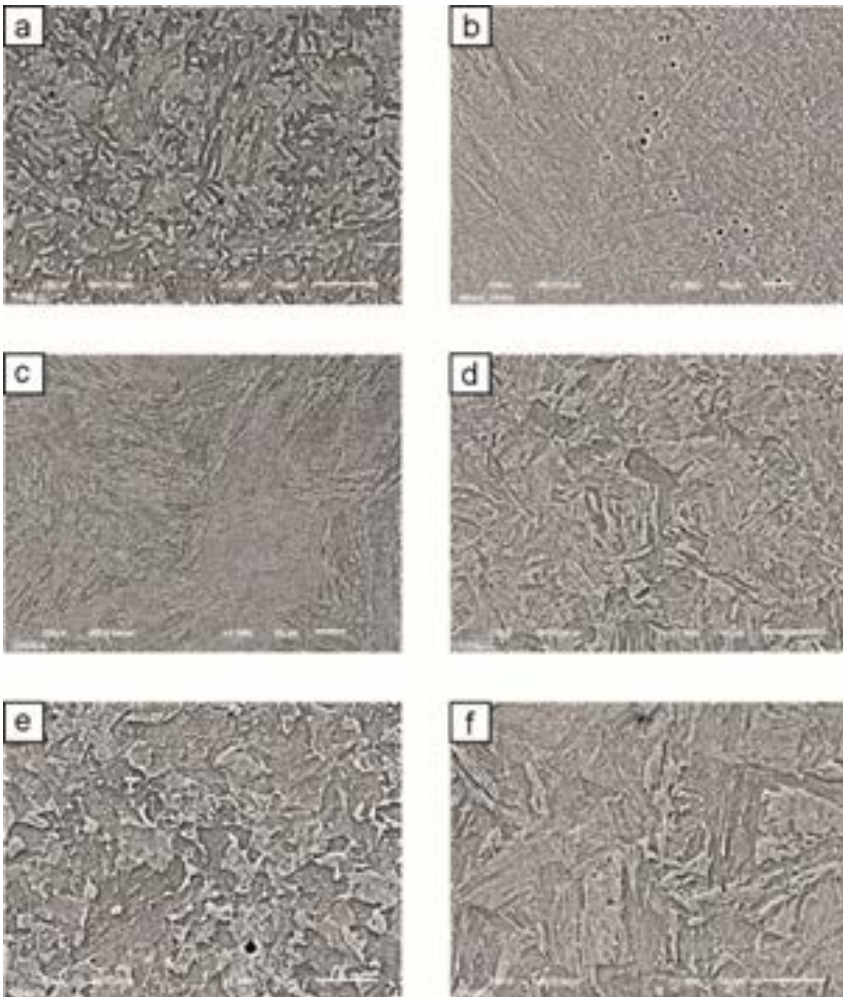

Fig. 9. Structure visible in the I-shaped welded joint: weld (a), fusion line (b), HAZ superheated area (c), HAZ normalisation area (d), HAZ partial normalisation area (e) and HAZ recrystallization area (f); etchant: Nital (3%)

Distribution of microhardness in the welded joint area

The assessment of the effect of the welding process on changes in the hardness of the joints required the performance of microhardness measurements. The measurements involved the use of the Vickers hardness test carried out under a load of 0.98 N. The tests enabled the determination of the distribution of hardness HV0.1. The test results concerning both types of the joints made of steel S960QL are presented in Figures 12 and 13. The measurement lines are presented in

BY-NC

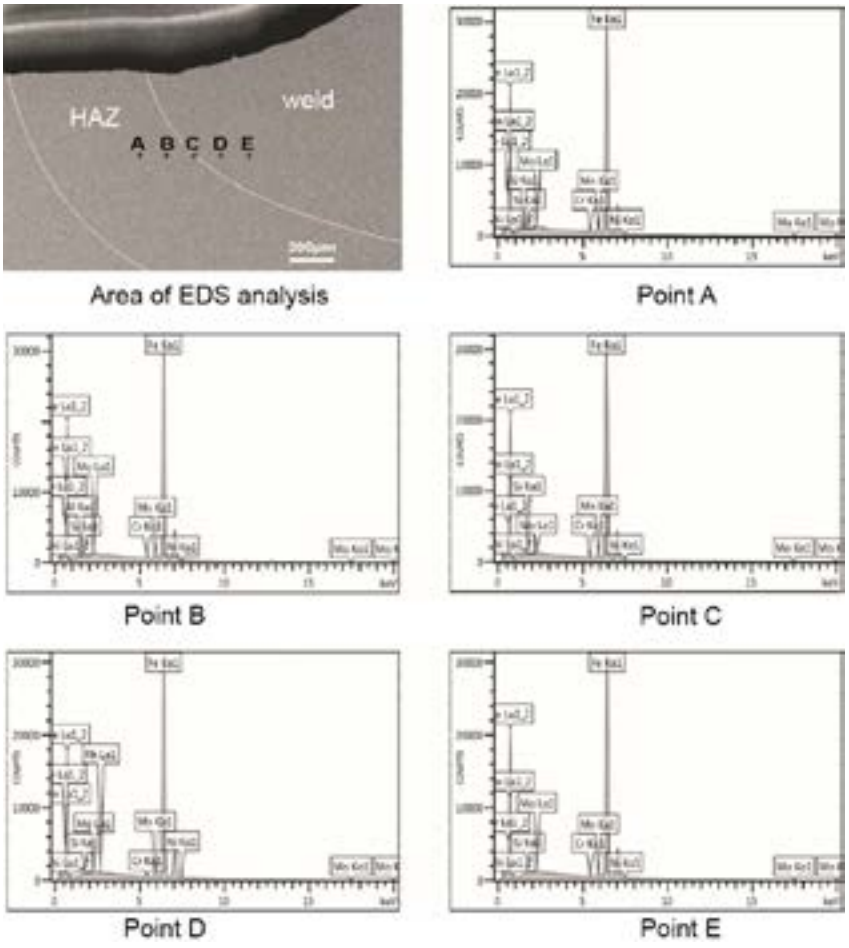

Fig. 10. X-radiation analysis results in relation to the fusion line of the I-shaped weld

Table 4. Contents of alloying elements in individual areas of the weld

Point	Contents of alloying elements [%]				
	Mn	Si	Ni	Cr	Mo
A	1.33	0.35	0.06	0.27	0.74
B	1.33	0.36	0.04	0.27	0.81
C	1.36	0.44	0.60	0.30	0.60
D	1.59	0.46	1.15	0.36	0.57
E	1.42	0.52	1.03	0.35	0.66

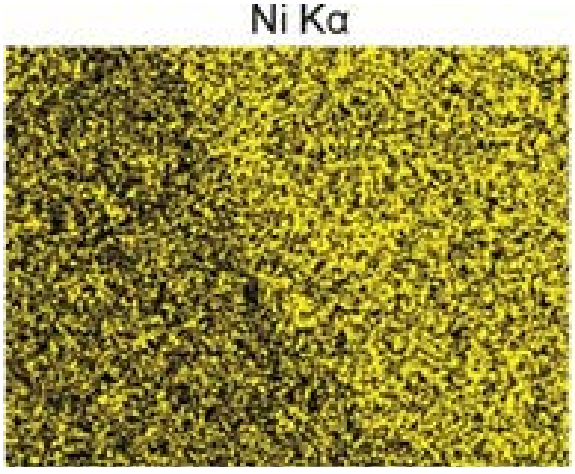

Fig. 11. Qualitative analysis of the distribution of Ni in the fusion line of the I-shaped weld

the miniatures of the joints, whereas the fusion line is marked in the diagrams.

Summary

In order to ensure the obtainment of the appropriate quality of welded joints it is necessary to use the filler metal characterised by the chemical composition similar to that of the material to be joined. However, in cases of high-strength steels, contents of alloying elements may vary significantly. The foregoing results from the fact that the weld should obtain appropriate strength. For this reason, depending on the strength of the filler metal, joints can be divided into three types, i.e. "matching", "overmatching" and "undermatching", where the strength of the filler metal is equal, higher or lower than that of the material subjected to welding. In the case under discussion the assessment was related to the joint of the matching type, i.e. where the value of the filler metal yield point was similar to that specified for steel S960QL and amounted to 930MPa. The carbon equivalent related to the base material amounted to 0.59 %, whereas that in relation to the filler metal amounted to 0.79 %. The above-named high values necessitated the adjustment of welding parameters leading to the reduction of a heat input so that it would not exceed 1 kJ/mm. However, the foregoing did not prevent the formation of hardened structure, the hardness of which in the fusion line reached 500 HV0.1 on the face side of the V-shaped weld.

The metallographic tests of the joint structure revealed its significant heterogeneity, with the ferritic-bainitic structure dominant in the joint area. The HAZ superheated area adjacent

BY-NC

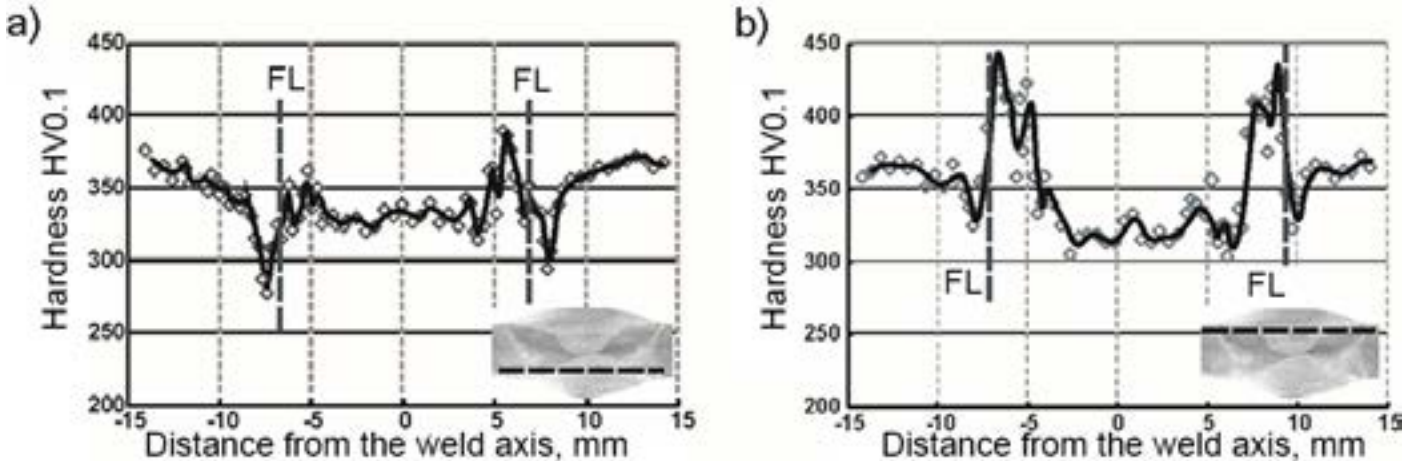

Fig. 12. Hardness measurement results in relation to the I-shaped weld made of steel S960QL: root side (a) and face side (b), FL – location of the fusion line

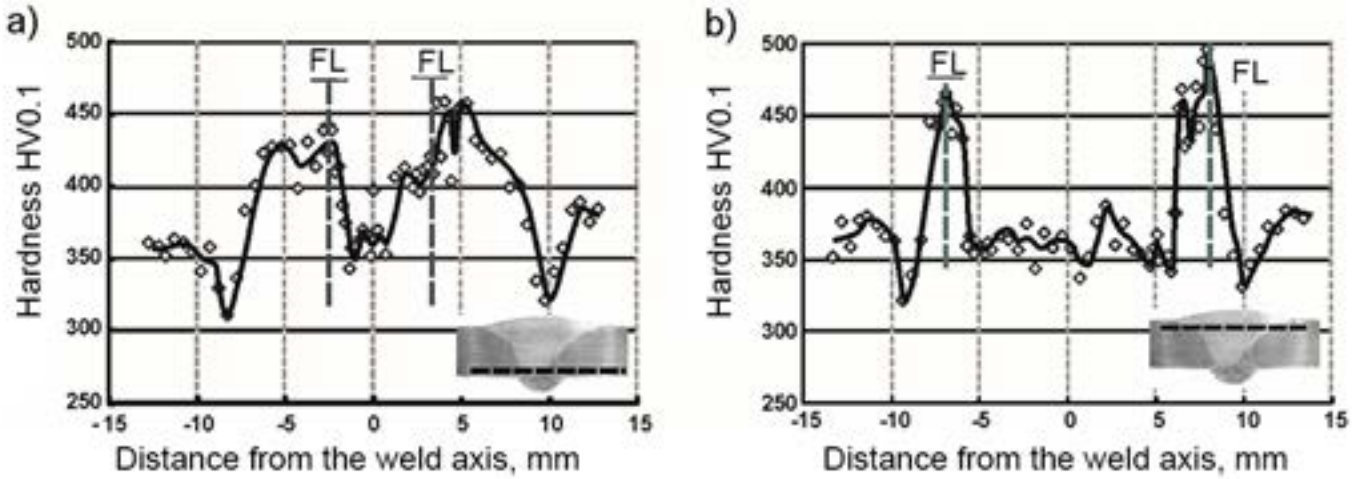

Fig. 13. Hardness measurement results in relation to the V-shaped weld made of steel S960QL: root side (a) and face side (b), FL – location of the fusion line

to the that of the fusion line was characterised by the significant grain growth, with grain diameters being restricted within the range of 50 μm to 60 μm. In the normalisation and recrystallization zones, the HAZ structure was similar to that of the base material. Certain porosity observed in the fusion line and in the weld could indicate the presence of traces of impurities on the surface of the plate edges.

The analysis of the chemical composition of the weld and that of the HAZ confirmed the differences in contents of alloying elements. The stirring of the molten filler metal wire with the partially molten edges of the base material resulted in the reduction of contents of alloying elements (expressed in %) in the weld (in relation to the filler metal). The carbon equivalent in the weld did not exceed 0.64% and was only slightly higher than the value specified in relation to the base material. The weld area contained nickel, chromium and molybdenum, i.e. alloying elements favourably affecting the strength and plastic properties of iron alloys.

The microhardness (HV0.1) measurements performed in the cross-sections of the butt joints with the welds having the I and V-shaped weld grooves revealed significant differences in hardness in relation to areas subjected to measurements and types of welds. In comparison with the V-shaped weld, the I-shaped weld was characterised by hardness lower by approximately 50 HV0.1. In the fusion line, hardness did not exceed 450 HV0.1. The hardness of the weld itself was restricted within the range of 320-330 HV0.1, i.e. by approximately 50 HV0.1 lower than the hardness of the base material. The hardness of the weld containing the V-shaped weld groove was similar to that of

BY-NC

the base material. The maximum hardness value in the fusion line amounted to 500 HV0.1. In addition, the tests revealed the positive effect of the second thermal cycle in terms of changes in the course and value of hardness in the first bead/root. Accompanying phenomena (tempering) led to the reduction of the gradient and the maximum hardness by approximately 50 HV0.1. All of the diagrams revealed the local reduction of hardness in the HAZ adjacent to the base material by a value restricted within the range of 30 HV0.1 to 50 HV0.1. The above-named area was the zone of incomplete normalisation, characterised by reduced mechanical properties. In the properly made joint, the above-named zone represented the weakest area of the joint, rupturing during the tensile test.

In conclusion it should be emphasized that martensitic-bainitic structural steels are very sensitive to the effect of welding thermal cycles. The processes triggered by welding were responsible for structural changes, including significant grain growth in the superheated area and structural heterogeneity in the remaining areas of the HAZ. At the same time, the aforesaid processes led to changes in hardness in the joint area and, consequently, to diverse mechanical properties in the heat affected zone. The comparison of the two types of joints subjected to the tests revealed that the butt joint with square butt weld preparation ("I-shaped") was characterised by more favourable parameters, including lower and more uniform hardness values, favouring higher formability of the weld.

References

[1] Lachowicz M., Nosko W.: Spawanie stali konstrukcyjnej Weldox 700. Przegląd Spawalnictwa, 2010, no. 1, pp. 13-18.

[2] Filary gigantów. Blacha gruba z Dillinger Hütte. [online], accessed on: 06.02.2018, http://stal.elamed.pl/material[24561].

[3] Jha A.K., Manwatkar S.K., Narayanan P.R., Pant B., Sharma S.C., George K.M.: Failure analysis of a high strength low alloy 0.15C–1.25Cr–1Mo–0.25V steel pressure vessel. Case Studies in Engineering Failure Analysis, 2013, no. 1, pp. 265–272, DOI: 10.1016/j.csefa.2013.09.004.

[4] Marecki P.: Badania niskocyklowej wytrzymałości zmęczeniowej połączeń spawanych mostu towarzyszącego ze stali wysokowytrzymałych. Rozprawa doktorska. Wojskowa Akademia Techniczna, Warszawa, 2012.

[5] Tokyo Gate Bridge. IDI Quarterly. Jap. Infrastructure Newsletter, 2012, no. 60, pp. 2-4 [online], accessed on: 07.02.2018, http://www.idi.or.jp/tech/quarterly/idi60.pdf.

[6] [online], accessed on: 14.02.2018, http://www.dnt.co.jp/english/results/img/index-ph12.jpg.

[7] Wińcza M.: Ekonomika produkcji spawanych konstrukcji stalowych. [online], accessed on: 07.02.2018, https://www.rywal.com.pl/vademecum/36-vademecum/inne/74-ekonomika-produkcji-spawanych-konstrukcji-stalowych.html.

[8] Makowieckaja O. K.: Obecna sytuacja na rynku głównych materiałów konstrukcyjnych i techniki spawalniczej, Biuletyn Instytutu Spawalnictwa w Gliwicach, 2011, no. 4, pp. 39-52.

[9] Butnicki S.: Spawalność i kruchość stali. WNT, wyd. 3 popr. i uzup., Warszawa, 1991.

[10] Blicharski M.: Inżynieria materiałowa. WNT, wyd. 3 zm. i rozsz., Warszawa, 2012.

[11] Zeman M., Sitko E.: Przegląd stali o wysokiej i bardzo wysokiej wytrzymałości, Biuletyn Instytutu Spawalnictwa w Gliwicach, 2013, no. 3, pp. 30-38.

[12] Recommendation for welding of XABO® 890 and XABO® 960.ThyssenKrupp Steel, edition 09/2004, [online], accessed on: 20.02.2018, https://www.thyssenkrupp-steel.com/media/content_1/publikationen/

BY-NC

grobblech_migration/n_a_xtra_xabo/verarbeitung/schweissen/recommendations_for_welding_xabo_890_960.pdf.
[13] SuperElso® 960. A High Yield Strength steel for welded and weight-saving structures. ArcelorMittal, 03.07.2012, [online], accessed on: 16.02.2018, http://solid.cl/SuperElso960.pdf.
[14] UNION X96. Böhler Welding by voestalpine, [online], accessed on:16.02.2018, http://www.alruqee.com/Userfiles/Product/TablePdf/19042016000000T_Union%20X%2096_solid%20wire.pdf.